Behavioural Processes 164 (2019) 38–47

Contents lists available at ScienceDirect

Behavioural Processes

journal homepage: www.elsevier.com/locate/behavproc

Particle motion and sound pressure in fish tanks: A behavioural exploration of acoustic sensitivity in the zebrafish

James Campbell[a], Saeed Shafiei Sabet[a,b], Hans Slabbekoorn[a]

[a] Institute of Biology Leiden, Leiden University, Sylviusweg 72, Netherlands
[b] Fisheries Department, Faculty of Natural Resources, University of Guilan, Sowmeh Sara, P.O. Box 1144, Iran

ARTICLE INFO

Keywords:
Captive behavior
Experimental exposure
Fish welfare
Noise impact
Sound measurement
Particle velocity

ABSTRACT

Underwater sound fields can be complex, both in open water and small tank environments. Here we measured 1) spatial variation in artificially elevated sound levels in a small fish tank for both particle motion and sound pressure. We confirmed that the ratio of pressure and particle motion deviated considerably from what would be expected in theoretical far field environments. We also tested 2) whether the acoustic response tendency of adult zebrafish (*Danio rerio*) was correlated to the sound field conditions at their position at the moment of sound onset. We found no correlation between the intensity, quality, or directionality of the behavioural response and the sound pressure or the directivity and ellipticity of particle motion. There was a negative correlation, however, between the tendency to freeze and the particle velocity level. The data and experimental setup provided here may serve a basis to further explore the acoustic world of fish in complex environments and may contribute to the study of potential welfare and conservation issues related to anthropogenic noise.

1. Introduction

Ship traffic, wind turbines, pile driving, and seismic exploration now represent significant components of underwater soundscapes worldwide (Andrew et al., 2002; Hildebrand, 2009). As all fish are capable of detecting sound, acoustic signals and environmental cues play an important role for many fish species in the context of reproduction, orientation and predator-prey interactions (Popper and Hastings, 2009; Slabbekoorn et al., 2010; Radford et al., 2014). The acoustic characteristics of human activities are typically broadband, more or less temporally structured, and biased towards relatively low frequencies. There is also often high structural similarity with biologically relevant sounds and large spectral overlap with the auditory sensitivity of fish. As anthropogenic sounds can be loud and propagate well through water, there is a growing concern about potentially detrimental effects and an increasing awareness about a general gap in fundamental insights about the acoustic world of fish (Williams et al., 2015; Kunc et al., 2016).

To examine the acoustic world of fish and gain understanding about the potential effects of anthropogenic noise, both outdoor and indoor experiments are employed (e.g. Neo et al., 2014, 2016; Simpson et al., 2015, 2016). While outdoor experiments provide a high degree of behavioral and acoustic validity, they tend to be challenging to implement and suffer from a low degree of controllability. Contrastingly, indoor experiments provide a high degree of control but lack acoustic and behavioral validity when compared to open water conditions (Slabbekoorn, 2016). While the acoustic differences between natural water bodies and relatively small tanks have been widely acknowledged (Parvulescu, 1964; Kaatz and Lobel, 2001), there remains a paucity of literature examining these differences from an empirical perspective (Kaatz and Lobel, 2001; Akamatsu et al., 2002). Furthermore, many fish spend time in shallow waters or in close proximity to surface, rock, and bottom boundaries, where the sound fields are more complex than in open water conditions and captive fish also experience sound fields in fish tanks that can be unintentionally or experimentally noisy.

While all fish are able to detect acoustic particle motion using a specialized structure called the otolith organ (Fay, 1984; Hawkins and Popper, 2018; Popper and Hawkins, 2018), fishes possessing a swim bladder are also able to detect the sound pressure component of sound through pressure-to-motion conversion via the air-filled cavity of the swim bladder (Popper and Fay, 2011). Specialized adaptations like the Weberian apparatus in Ostariophysians can further enhance the acoustic sensitivity to sound pressure by acting as an efficient conduit for kinetic energy between the swim bladder and the inner ear. These specialized adaptations can increase the frequency range and decrease absolute hearing thresholds (Schulz-Mirbach et al., 2012).

Previous studies have assessed hearing thresholds and acoustic response tendencies in fish (Popper and Fay, 1973; Horodysky and Brill,

E-mail address: jamesadamcampbell@gmail.com (J. Campbell).

https://doi.org/10.1016/j.beproc.2019.04.001
Received 25 September 2018; Received in revised form 1 April 2019; Accepted 1 April 2019
Available online 03 April 2019
0376-6357/

2008). Many of these studies are done in laboratory facilities and with the fish close to the surface in a small tank which complicates the interpretation and comparison of results. It is therefore wise to treat absolute acoustic measures from such studies as study-specific and not as general truth. However, relative sensitivity information across the spectrum should also be treated with care, as this involves the outcome of overlapping ranges of sound reception through both particle motion and sound pressure, for which the sound field conditions are highly variable with dynamic ratios between the two components under typical indoor fish tank conditions (Parvulescu, 1964; Rogers and Cox, 1988). Some studies have compared fish hearing thresholds for particle motion and sound pressure by isolating these acoustic components within the experimental setup and exposing fish to acoustic signals comprised exclusively of either particle motion or sound pressure (Bretschneider et al., 2013; Wysocki et al., 2009). Although these studies revealed some more advanced insights into fish auditory perception, there remains especially little knowledge regarding how fish react behaviourally when exposed to variable ratios of the two components.

Although many fish do not reside in far field, open water acoustic conditions, this is still a useful point of reference for exploring more complex sound fields. In these conditions, a propagating sound shares a fixed relationship between its sound pressure and particle motion components, thus the predicted far-field particle velocity (PFV) for a given sound pressure measurement can be calculated using Eq. (1) along the direction of propagation:

$$PFV = \left(\frac{rms(p_{measured})}{c \cdot \rho}\right) \tag{1}$$

where $rms(p_{measured})$ is the root mean square of the measured sound pressure over time, c is the speed of sound in water, and ρ is the density of water.

While the relationship between sound pressure and particle motion under these conditions is generally constant, most small tank experiments are conducted in the acoustic near-field due to the relatively long wavelengths of the frequencies of interest with respect to the dimensions of the tanks used. In the near field tank environment, sounds are expected to express relatively higher levels of particle motion as compared to far-field conditions (Bretschneider et al., 2013). Additionally, small tanks typically act as shallow water waveguides where frequencies above a cutoff will propagate as normal modes, comprised of constructively interfering surface/bottom reflections, and those frequencies below the cut-off will attenuate rapidly. When viewing a tank as a shallow water waveguide where the water surface and tank bottom are pressure release boundaries, lower levels of sound pressure and higher levels of particle motion are expected to be measured in close proximity to these boundaries (see Akamatsu et al., 2002; Gray et al., 2016).

A critical parameter of the sound field to understand behavioural response patterns is the directionality of the particle motion (Schuijf and Buwalda, 1975; Popper and Fay, 1973; Rollo and Higgs, 2008). In a far field environment with a single monopole sound source, acoustic particle motion directionality is observed as the oscillation of water particles along the direction of the propagating wave. However, under spatially restricted conditions such as small tanks, fish are continuously exposed to reflected sound waves which interfere with each other. When two sound waves of a given frequency with different trajectories pass through a common point, the directional components of both waves will be summed in the resulting particle motion. Additionally, the phase difference between the waves can cause a two- or three-dimensional oscillation of particles which can be characterized by what we term particle ellipticity. Here, we broadly define particle ellipticity in two dimensions as the ratio of the length of the major axis of particle displacement over the length of the axis perpendicular to the major axis of particle displacement (Fig. 1).

Current models of fish hearing are based on the assumption that fish

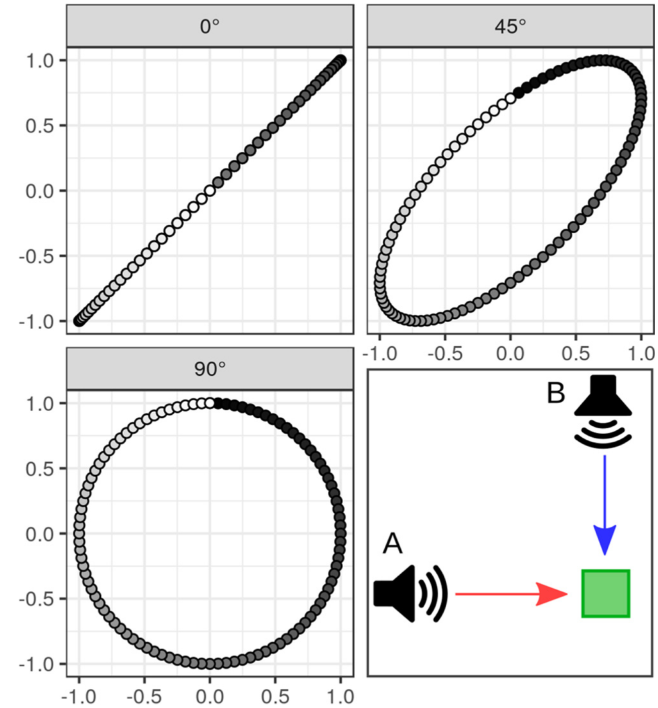

Fig. 1. A visual illustration of particle ellipticity. In this simple example, if speakers A and B both play a pure tone of the same frequency, the expected trajectory of particle motion within the green area will be defined by the phase difference between the signals upon arrival. In the first three panels, the expected instantaneous particle displacement for phase differences of 0, 45, and 90° are shown with the color of the circles representing the time of measurement. The resulting elliptical pattern of displacement which is a function of the phase difference between interfering signals is what we refer to as particle ellipticity in this article.

determine the direction of sound propagation through acoustically induced otolith motion along the axis of the acoustic wave (Rollo and Higgs, 2008). As points in an acoustic field with high particle ellipticity will result in otolith motion that deviates from a single axis of displacement, this implies that high degrees of particle ellipticity may undermine the ability of fish to localize sounds. Some studies have examined the directional components of particle motion in localization experiments (see Dale et al., 2015) and Zeddies et al. (2012) implicitly provided evidence of a species localizing in a field containing areas of relatively high particle ellipticity. To our knowledge, no studies have quantitatively examined the role of particle ellipticity in sound source localization.

Here we conducted two studies in a relatively small tank: one in which we measured particle motion and sound pressure levels to explore the relationship between the two sound components in a fish tank and a second to explore the potential relevance of variation in the acoustic parameters for the behaviour of experimental fish. The first descriptive study examined how the ratio of sound pressure to particle motion in a small tank varies in response to the spatial location within the tank as compared to theoretical open-water conditions. In the second experimental study, we further examined the sound pressure and particle motion components within the context of an acoustically induced behavioural response study using zebrafish (*Danio rerio*). We examined the 1) *occurrence*, 2) *intensity*, and 3) *direction* of acoustically elicited fast start responses for individual fish with respect to the predicted sound pressure and particle motion conditions they would have experienced at their location during the on-set of sound exposure. We expected high levels of either sound pressure or particle motion to contribute to an increased tendency and intensity for a behavioural response and that the directionality of startle responses would be correlated to the directionality of particle motion.

2. Methods

2.1. Descriptive study 1

2.1.1. Experimental setup

The experimental tank used in the present study was constructed from glass and had the following dimensions: 100 × 50 × 50 cm, a wall thickness of 0.75 cm, and a water depth of 40 cm. The tank was positioned on a table on top of ˜4 cm of acoustic insulating material to reduce acoustic artifacts caused by building vibrations. Within the tank, the acoustic field was measured along a three-dimensional grid at 10 cm increments using a custom-built vector sensor comprised of three orthogonality oriented geophones encased in a negatively buoyant, epoxy sphere (Bretschneider et al., 2013; Shafiei Sabet et al., 2015). A 10 cm grid was chosen based on the size of the vector sensor so measurements would not be spatially overlapping. The vector sensor was positioned along this grid using two perpendicularly oriented red lasers (λ = 635 nm in air). The negatively buoyant vector sensor was suspended in the water by two nylon wires. This system allowed us to position the vector sensor within a ˜1 cm range of accuracy. All measured positions in this grid were at least 10 cm away from the tank walls.

The tank was ensonified using a JBL EON500 in-air speaker (USA, Maximum volume, Equalizer: Boost) connected to a DR-05 handheld recorder (Tascam, USA) at a distance of 1.5 m with the speaker facing the center of one of the two widest walls of the tank. During each acoustic measurement, the experimental tank was ensonified with 10 s of white noise. 10 s was chosen to provide ample time to calculate root-mean-square sound levels. The white noise playback track was artificially generated in Audacity (http://audacityteam.org/, version 2.0.5) and a bandpass filter was applied between the frequency range 100–1000 Hz (48 dB roll-off per octave) resulting in a signal that broadly covered the more sensitive hearing ranges of many fish species (see Popper and Fay, 2011). The playback volume of the in-air speaker was adjusted so that a sound pressure level (SPL) of 112 dB (re 1uPa) was measured over 10 s in the center of the tank with a calibrated HTI 96-min hydrophone (High Tech, USA) connected to a DR-100MKII recorder (Tascam, USA). In this experimental setup, we could not raise the speaker volume any louder without disturbing nearby colleagues.

In addition, a supplementary set of measurements was taken to investigate the effect of variable speaker volume where the vector sensor was placed in the vertical center of the tank, 14 cm away from the wall closest to the speaker. The tank was then ensonified with the same white noise exposure 21 consecutive times while the vector sensor remained in the same position, with each exposure digitally set to be 2 dB quieter than the previous.

2.1.2. Acoustic measurements

All sound pressure and particle motion measurements were recorded with the custom-built vector sensor and amplifier that was previously used in studies by Bretschneider et al. (2013) and Shafiei Sabet et al. (2015). This was then connected to a Picoscope 3425 USB Oscilloscope (Pico Technology, England & Wales) and data was logged from the oscilloscope using a program written in Visual Basic for Applications within Microsoft Access 2010 (Microsoft, USA).

The vector sensor was calibrated in reference to a M20 directional hydrophone (Geospectrum Technologies Inc., Canada). This model of sensor has been used in other underwater sound impact studies (Simpson et al., 2016; Morris et al., 2018; Neo et al., 2016) and the manufacturer, Geospectrum, provided us with the calibration values. The calibration of the sensor used in this experiment was conducted by suspending the reference M20 directional hydrophone in the center of the large tank and ensonifying the tank with an in-air speaker 1.5 m away with broadband white noise for 10 s. The M20 directional hydrophone was then replaced by the custom-built vector sensor and the exposure was repeated. By comparing the resulting measurements from the two devices in the frequency domain we were able to construct a receiver sensitivity graph for each channel of the custom-built vector sensor. As the acoustic environment in the experimental tank is prone to unwanted acoustic artifacts and the differing size of the sensors results in unequal sampling areas, a degree of inaccuracy is to be expected from this calibration method. To compensate for this, we repeated the calibration five times in the same tank. Each repeated calibration required removing and re-suspending the sensors in the calibration tank. Repeated calibrations revealed variations in calibrated values above 1000 Hz of more than two decibels, resulting in a final calibrated range of 50–1000 Hz.

2.1.3. Acoustic analysis

All audio analyses were conducted using Matlab (Mathworks, USA, Version 8.1) with a bandpass filter applied between 100–1000 Hz (within the calibrated range of our vector sensor) and following the standardized definitions for each measurement as seen in (Ainslie, 2011), unless otherwise specified. Particle velocity measurements were reported as sound velocity level (SVL), and are defined according to Eq. (2):

$$SVL = 20 \cdot log_{10}\left(\frac{rms(u_{measured})}{u_{reference}}\right)\text{dB}, \tag{2}$$

where $rms(u_{measured})$is the vector sum of the measured root mean square of the particle velocity over time across all axes and $u_{reference}$ is the referenced particle velocity (1 nm/s).

To compare SVL and SPL measurements in a context relevant to open water experiments, we examined the excess SVL. This measurement was calculated by taking the ratio of the measured particle velocity under far field, open water conditions (Eq. (1)) over the expected particle velocity as calculated from the paired pressure measurements in the tank as shown in Eq. (3):

$$ExcessSVL = 20 \cdot log_{10}\left(\frac{rms(u_{measured})}{PFV}\right)\text{dB}. \tag{3}$$

Under far-field open water conditions, SPL is expected to show no relationship with excess SVL, and as a result, excess SVL measurements taken in these conditions would be expected to be 0 dB. Excess SVL measurements taken in environments where relatively higher ratios of particle motion to pressure are expected, such as the near-field of a sound source or in close proximity of a pressure release boundary, will result in excess SVL values greater than 0 dB.

2.1.4. Statistical analysis

All statistical analyses were carried out in R (version 3.2.2, including the packages: ggplot2, nlme, lme4, MASS, and CircStats). We examined the relationship between the spatial parameters (i.e. the position of the vector sensor in the tank) of each acoustic measurement and the resulting SPL and SVL values in the experimental tank using Generalized Linear Models assuming a Gaussian error distribution. The selection of variables used in each model was determined by Akaike information criterion (AIC) stepwise selection (both directions). The spatial variables included in the model selection were the continuous variables: *distance from the tank wall closest to the in-air speaker, distance from the closest tank wall facing the direction adjacent to sound propagation (including the second degree orthogonal polynomial), distance from the bottom of the tank* and the binomial variables: *close to tank bottom or water surface* and *close to either wall facing the direction of sound propagation*.

For examining the relationship between Excess SVL and the spatial variables, we again used a Generalized Linear Model with assumed Gaussian error distribution. The variables used for the model selection are the same as used in the SVL/SPL comparison, except for the

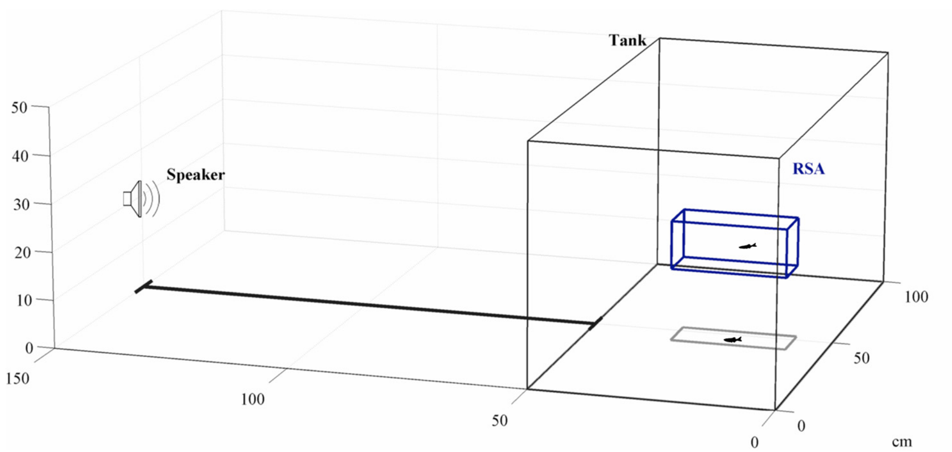

Fig. 2. An overview of the setup for the startle response experiment. The tank was filled to a depth of 40 cm with water and the blue rectangle within the tank represents the restricted swimming area (RSA): A metal frame covered in soft plastic wrap. The RSA confined the experimental fish to an area of the tank where we had measured variable particle motion to pressure ratios while allowing us to track the individual with two adjacently placed cameras. Pilot measurements with and without the RSA present showed no effect of the RSA on the acoustic field.

addition of *SPL* as a fixed effect and the use of Excess SVL as the responding variable.

2.2. Experimental study 2

2.2.1. Experimental setup

The behavioural response experiment was conducted in the same in-air speaker tank setup as in experiment 1, with the exceptions that the speaker was placed 1 m away instead of 1.5 m so higher in-tank sound levels could be achieved. Additionally, a restricted swimming area measuring 24 × 10 x 10 cm was placed within the glass tank to constrain the fish to a small area where we had previously measured highly variable particle motion to sound pressure ratios (Fig. 2). We then remeasured the sound field within this restricted swimming area (Fig. 3).

The restricted swimming area was constructed from a rectangular iron frame with walls made of plastic wrap. Plastic wrap was chosen because of its visual and acoustic transparency. During the pilot trial, a comparison of measurements taken in the same positions both with and without the restricted swimming area surrounding the sensor resulted in no observable difference in SPL or SVL measurements. Two HC-V500 video cameras (Panasonic, Japan) set to record at 50 fps(interlaced) were placed above and to the side of the tank to obtain a dorsal and lateral view of the individuals during exposures. The volume level of the DR-05 handheld recorder attached to the EOS500 loudspeaker (Maximum volume, Equalizer: Flat) was adjusted in this behavioural experiment to achieve an SPL of 120 dB in the center of the tank with a 10 s duration playback of white noise bandpass filtered between 10–2000 Hz. A wider frequency range was used in this experiment so the sound exposure would cover the whole zebrafish hearing range which is known to exceed 1000 Hz (Higgs et al., 2002) and the 120 dB sound level was chosen based on a pilot trial where this level was shown to readily illicit startle responses in zebrafish. Playback tracks used in this experiment consisted of a one-hour period of silence followed by 10 one-second pulses (white noise, 10–2000 Hz) randomly distributed over a three hour period. The random placement of the pulse noises was determined by dividing the three hour trial period into 10 segments of 18 min. A pulse was then played at a randomly selected minute within each 18 min segment.

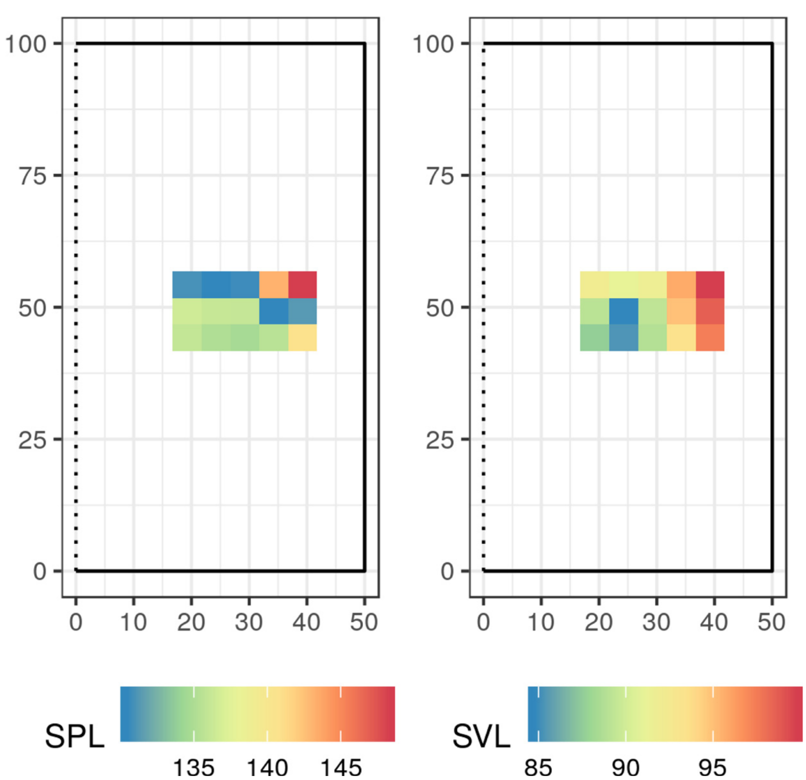

Fig. 3. SPL (left) and SVL (right) measurements along a horizontal plane within the RSA. Measurements were made along a 5 cm grid, resulting in some overlap between adjacent sample locations due to the size of the sensor used. Black lines represent the tank walls while the dotted black line indicates the tank wall closest to the speaker. SPL and SVL measurements are calculated with respect to the reference values of 1µPa and 1 nm/s, respectively.

Once the water was warmed to at least 22 °C, the trials began by placing an individual into the restricted swimming area within the large tank and the playback track was started after the video cameras had begun recording. The start and end temperatures were recorded for 12 of the 14 trials and tank heaters were removed during the trials. Temperatures ranged from 22.5 to 24 °C upon the start of each trial and the maximum drop in temperature by the end of a trial was 1.5 °C. In addition, the room hosting the experiment had no windows, thus lighting conditions could be kept consistent throughout all the trials. A LUNASIX F light meter (P. Gossen & co, Erlangen, Germany) was used to measure the experimental light conditions by placing the light meter 5 cm above the water surface in the horizontal center of the tank, resulting in an illuminance of 1290 lx. Upon the start of the playback track, we left the room and did not return until after the 4 h trial period had ended. Because of moderate but regular background noise and vibrations due to nearby building maintenance during the morning and early afternoon, all trials were initiated between 15:45 − 16:40 and we only conducted one trial per day.

2.2.2. Behavioural analyses

Each trial had a unique timing pattern for sound exposures and we assessed the spatial position of the fish at each pulse moment in the trial sequence. For each sound exposure, one minute of video before and after the onset of each pulse was extracted for analysis and converted to a Motion-JPEG video format (50 frames per seconds, progressive scan) using FFmpeg (https://www.ffmpeg.org/, version 2.4). Location tracking of the individuals was then conducted in Matlab using a background subtraction algorithm based on greyscale values. The results of the motion tracking algorithm were reviewed and tracking errors were manually corrected. We then combined the information from the dorsal and lateral cameras to provide three-dimensional spatial position data for individuals before and after sound exposures. Example output of the spatial tracking analysis can be seen in Fig. S1.

We used the video recordings to score behavioral states related to swimming speed, fast start onset, and freezing. The presence of and onset of distinct fast start responses were defined by any sudden quick movement which followed the first and second stage motions associated with fast start responses in zebrafish (Mirjany et al., 2011). Freezing was defined by interruption of all activities except breathing (Shafiei Sabet et al., 2016) for at least 10 s. We scanned for fast start responses ranging from 2 s before and after the onset of the sound exposure. In circumstances where a fast start response was suspected but not clearly obvious to the observer, these were treated as expressing no fast start response. The acoustic conditions of each potential startle response were determined independently and after behavioural assessments and the scoring by the observer can thus be regarded blind to the treatment.

To collect more precise directional information during the startle response, the midline of the individual was traced manually over a period of 1 s before and after the startle response along the horizontal plane. The midline was defined as a straight line drawn from the snout of the fish to the midpoint between the pectoral fins (Mirjany et al., 2011). Because of the low temporal resolution of the video footage, the midlines could not be quantified accurately in three-dimensional space. Consequently, only the dorsal camera was used to analyze the directional component of the startle responses.

2.2.3. Quantifying the acoustic field at startle response locations

The acoustic field in the restricted swimming area was measured with the same calibrated vector sensor as used in experiment 1. The area enclosed by the restricted swimming area was measured along a horizontal plane at 5 cm increments at the vertical center of the restricted swimming area at a 20 cm water depth (Fig. 2). While a 5 cm grid resulted in spatial overlap of measured particle motion values, this measurement scheme was chosen due to the relatively small size of the RSA and the expectation that the sound field would be more spatially variable in this section of the tank. The measured acoustic field values of SPL, SVL, and the direction of particle motion were then linearly interpolated to predict the acoustic values at the exact locations of the startle responses (Fig. 3). Due to the flexible nature of the plastic wrap walls and the small degree of error in the video tracking, when the fish were close to the walls of the restricted swimming area during the onset of noise exposure some tracking positions resided outside of the measured sound field and could not be interpolated. These points were excluded from the analysis.

To calculate particle ellipticity, the paired measurements of particle velocities for the X and Y channels of the vector sensor were plotted in a bivariate histogram (Fig. S2). As only the dorsal camera was used for tracking the directional component of the startle response, particle ellipticity was only calculated on the X–Y plane. Bivariate histograms were calculated over a period of 4 s during playback of white noise, band-pass filtered between 50–1000 Hz. A convex hull was then drawn around all values which were greater than 25% of the maximum frequency in the histogram. Particle ellipticity was then calculated by comparing the length of the major axis of the convex hull to its perpendicular axis using Eq. (4):

$$ParticleEllipticity = arctan\left(\frac{l_{adjacent}}{l_{major}}\right)\cdot\left(\frac{180}{\pi}\right) \tag{4}$$

Where l_{major} and $l_{adjacent}$ are the lengths of the major and adjacent axes of the convex hull, respectively, and the particle ellipticity is returned in degrees.

2.2.4. Statistical analysis

The effect of sound field components on the intensity of fast start responses was examined with a Linear Mixed Effects Model (maximum likelihood) with a Gaussian error distribution to predict the post-exposure average swimming speed and a Generalized Linear Effects Model with a Binomial error distribution to predict the probability of a freezing response within 50 s after the exposure. A visual check of residual plots was used to confirm that the assumptions of normally distributed residuals were met. In both models, the individual was defined as the random effect (random intercept) and the average swimming speed was calculated over a period of 10 s before and after the onset of noise exposure.

We determined the inclusion of the following fixed effects by AIC stepwise selection: SVL at the fish's location during the onset of noise exposure, SPL at the fish's location during the onset of noise exposure, exposure number, and the average swimming speed before the onset of noise exposure. A linear regression analysis was used to explore collinearity between the paired SVL and SPL estimates, but the relationship was not significant. The fixed effect expression of freezing behavior before the onset of noise exposure was also included in model construction to distinguish between cases in which the fish was swimming normally prior to the sound exposure and then froze in response to it, as opposed to a false detection when the fish was already in a frozen state before the exposure and remained frozen during and after the exposure.

Predicted SVL and SPL values at the individual's location during the onset of noise exposure were also compared to the occurrence of startle responses and the change in post-exposure swimming speed, but no correlations were evident. The final mixed effects models only included exposures that resulted in visible startle responses and the marginal and conditional R^2 values for each model were calculated according to Nakagawa and Schielzeth (2013), where the marginal R^2 represents the variance explained exclusively by the fixed effects and the conditional R^2 represents the variance explained by the combined fixed and random effects.

Circular statistics were employed to examine if there was a directional response related to the sound-field properties during the startle responses. The direction of escape during the fast start response over the temporal scales of 1, 2, 3, 4, and 5 frames (Each frame is spaced 20 ms apart) after an observed response was compared to the direction of particle motion analyzed over the bandwidths of 50–150 Hz, 150–250 Hz, 350–450 Hz, and 750–850 Hz. Because the mechanism which fish use to determine the acoustic directionality of particle motion is poorly understood, we treated the direction of escape as a diametrically bimodal distribution in which a value of 0 radians represents the fish swimming in either direction parallel to that of acoustic particle motion and a value of π radians as a direction perpendicular to that of particle motion.

2.2.5. Ethical approval and experimental animals

A total of 15 zebrafish were used in the experiment, one of which was exclusively used for a pilot trial. The fish were obtained from a commercial fish breeder. While the exact rearing conditions are not known to us, the zebrafish used in this experiment are likely to have been exposed to varying levels of anthropogenic noise which are typical of aquaculture facilities (see Craven et al., 2009). All experiments were performed in accordance with the Netherlands Experiments on Animals Act (DEC approval no: 10,069) that serves as the implementation of the Directive 86/609/EEC by the Council of the European Communities regarding the protection of animals used for experimental and other scientific purposes (1986).

3. Results

3.1. Descriptive study 1

3.1.1. SVL and SPL

The SVL and SPL components of the measured sound field followed generally similar spatial trends within the tank (Fig. 4) with a range of 20 dB for SVL and 35 dB for SPL. Most notably, the sound levels in the center of the tank were approximately 5 dB lower for SVL and 10 dB lower for SPL, as compared to locations close to both tank walls. For both SPL and SVL, measurements close to the surface were lower relative to the middle or bottom of the water column. There were no significant interaction effects in the SPL model, but we found a highly significant interaction effect in the SVL model between the *distance from the wall closest to the in-air speaker* and the *distance from the bottom of the tank* (T_{53} = -6.98, $p < 0.001$). A summary of the model results can be found in table S1.

Trends in excess SVL measurements relative to the spatial positions within the tanks were generally similar to those observed in the SVL and SPL measurements, as the excess SVL is calculated from both SVL and SPL. In addition, SPL showed a highly significant negative correlation with excess SVL (T_{48} = 49.6, $p < 0.001$). A summary of the statistical results can be found in table S2 and an overview of the measurements in figure S3. A supplementary set of measurements taken while the vector sensor was stationary, and the volume of the playback track was adjusted support these results (Fig. S4). Observed excess SVL values ranged from −15.1 to 16.2 dB across all sampling positions, with relatively higher excess SVL values closer to the water surface and bottom.

3.2. Experimental study 2

The mixed effects model predicting post-exposure swimming speed revealed that the *pre-exposure swimming speed*, *pre-exposure freezing behavior*, and *exposure number* were significantly correlated with a decrease in the *change of swimming speed*, although a majority of the explained variance was accounted for by the random effect of the individual ($R_c^2 - R_m^2 = 0.28$). SPL and SVL were not significantly correlated with a change in swimming speed. The test results are summarized in Table 1 and illustrated in Figs. 5 and 6.

The mixed effects model predicting the probability of a freezing response within 50 s after noise exposure revealed that higher SVL measurements resulted in a lower probability of a post-exposure freezing response while SPL showed no relationship. In addition, the average pre-exposure swimming speed was also negatively correlated with the probability of a freeze response. A majority of the variance was accounted for by the random effect of the individual ($R_c^2 - R_m^2 = 0.47$). The test results are summarized in Table 1 and illustrated in Figs. 5 and 6.

Rayleigh's test (mean direction alternate hypothesis) and Watsons test of uniformity showed that the direction of escape was not significantly different than that of a uniform circular distribution, except in the temporal range of 5 frames after the first observed startle motion and over a bandwidth of 750–850 Hz (Rayleigh's test: mean resultant length = 0.044, p-value = 0.011; Watsons test: U^2 = 0.182, p-value < 0.1). A one-tailed binomial test was then done on the non-uniform distribution to determine that there was a significant preference to escape in a direction parallel to that of particle motion (X^2 = 2.769, p-value = 0.048). A Watson's two-sample test was further used to check if the resulting distribution fitted a von Mises distribution, but the results were not significant. Predicted particle ellipticity values at the locations of the individual during the onset of sound exposure varied considerably over space and measured bandwidth (Fig. 7) and generally expressed higher values than what would be expected in ideal far field, open water conditions suggesting a complex sound field strongly influenced by reflected sound waves.

4. Discussion

Through the quantitative description of fish tank sound fields in the context of an acoustic response experiment, our results provide new insights into the sound field complexity of relatively small aquaria by introducing a metric, particle ellipticity, as a measure of directionality in particle motion. Experiment 1 showed that the SVL and SPL components of the sound fields within the experimental tank followed generally similar trends with relatively high SVL and SPL close to tank walls, regardless of speaker position, and relatively low SVL and SPL close to the surface. Furthermore, the excess SVL deviated well above and below theoretical far field, open water conditions with high SVL levels observed close to the water surface and tank bottom. In experiment 2, a general lack of correlations between acoustic and behavioural measurements such as speed and direction of the swimming response were observed. Additionally, high degrees of particle ellipticity were estimated at a majority of fast start locations. However, locations with higher SVL values during noise exposure were correlated with a lower probability of a post-exposure freezing response.

4.1. Fish tank acoustics

Our acoustic measurements confirmed that SPL, SVL, and excess SVL in small tanks are highly variable across spatial locations. The spatial and temporal variability observed in our setup stray considerably from the theoretical values that are expected to be experienced by fish swimming in far field, open water conditions. Consequently, indoor sound field assessments and behavioural response studies can be valuable to gain fundamental understanding about underwater acoustics and insights into housing conditions of fish in captivity, but they are unlikely to shed much light on free-ranging fish in outdoor conditions. Nevertheless, many fish occur in natural habitat with more complex sound fields. In this context, insights from indoor experiments can provide insight for sound impact on fish in shallow waters, close to surface, rock or bottom, so long as the experimental sound fields are appropriately described.

Sound pressure and particle motion measurements reveal several interesting findings, some of which were unexpected. The relatively low levels of SPL observed close to the water surface in our tank and high levels of Excess SVL close to the water surface and tank bottom are in line with our expectations of being near a pressure release boundary. However, we also expected relatively high levels of particle motion at the surface and that is not reflected by our measurements.

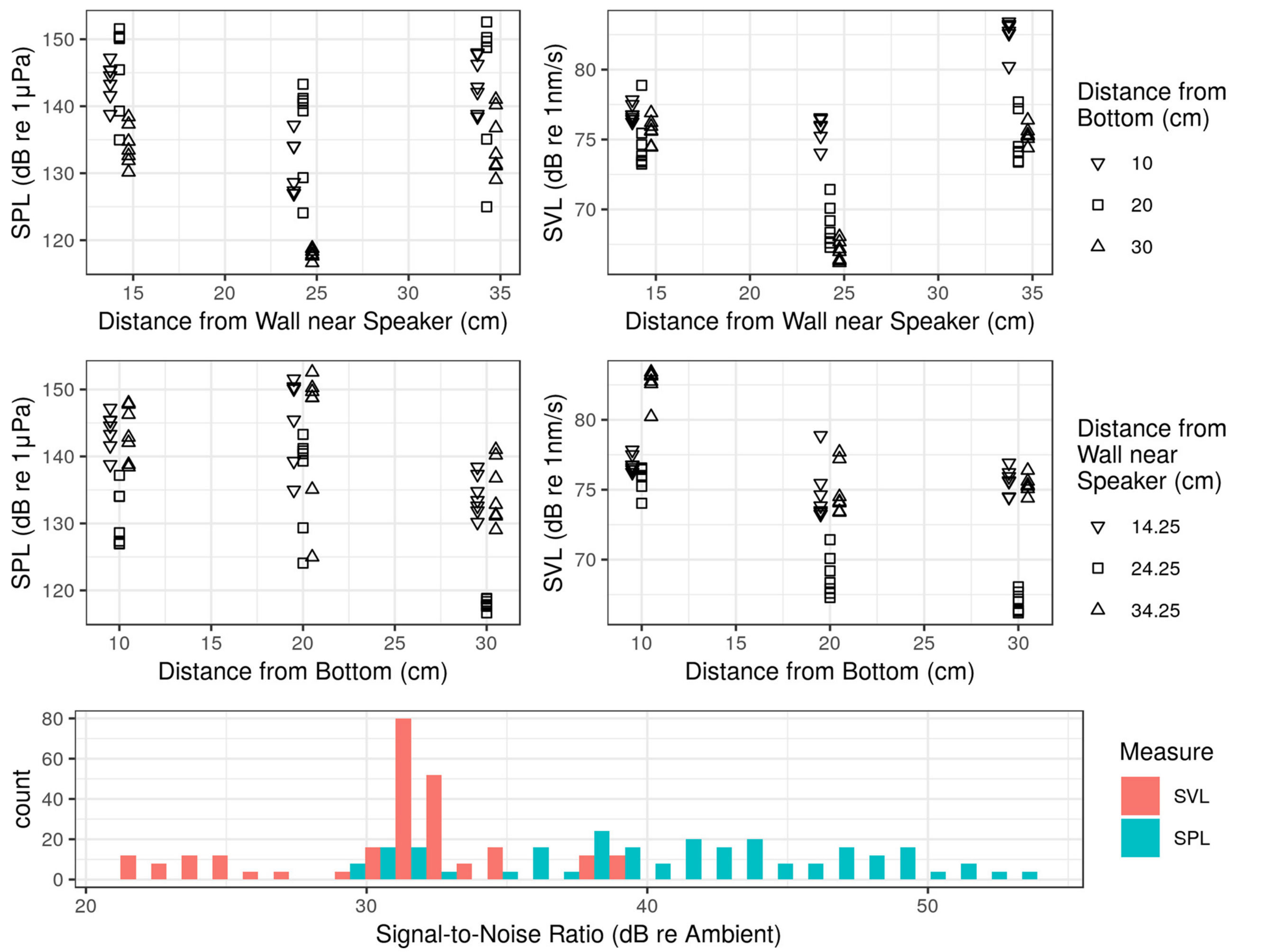

Fig. 4. SPL and SVL measurements in the big tank during white noise playback, bandpass filtered between 50 and 1000 Hz. Both components follow roughly similar trends across spatial locations within the tank. The bottom panel shows a histogram of signal to noise ratios for all SPL and SVL measurements.

We also observed higher SVL and SPL values closer to the bottom and closer to either tank wall, largely independent of the speaker location. While understanding the physical mechanism responsible for this observation is beyond the scope of the analysis and measurements presented here, it suggests the pressure and velocity intensity gradients of the tank sound field are not likely to carry accurate information about the location of the in-air speaker. Furthermore, high degrees of particle ellipticity found in the center of the tank indicate that the particle motion is an unreliable indicator of the location of the in-air sound source.

Some acoustic variation along the direction of in-air sound propagation was observed. Measurements taken close to both the bottom of the tank and the wall closest to the in-air speaker resulted in higher SVL measurements and a significant interaction effect between horizontal and vertical variation. As this interaction effect is only visible very close to the tank boundaries and is absent for SPL, it may result from the differing sizes of sampling areas between the hydrophone (~1–2 cm diameter) freely hanging in the center of the vector sensor and the geophones mounted within our vector sensor (9.5 cm diameter). Due to this size difference, the particle motion component of the vector sensor is sampling approximately 3.5 cm closer to any given sound source across all locations as compared to the paired samples from the hydrophone.

Table 1
Summary statistics for the mixed models comparing average swimming speed before and after noise exposure and the probability of a freeze response to SPL and SVL (n = 99). Only those sound exposures which resulted in a clearly observable startle response are included in the analysis.

Post-exposure Average Swimming Speed			Probability of Post-exposure Freeze response		
Fixed effect	Coefficient	*t*-value	Fixed effect	Coefficient	*z*-value
Intercept	11.59	5.39***	*Intercept*	−22.71	−2.22**
Exposure Number	−0.51	−2.60*	SVL	−0.29	−2.45*
Average swimming speed before exposure	0.48	1.87.	Average swimming speed before exposure	−0.64	−2.61*
Expression of freezing behavior before exposure	−2.57	−2.13*			
	R^2_m	R^2_c		R^2_m	R^2_c
	0.15	0.43		0.32	0.79

*** p-value < 0.001; * p-value < 0.05;. p-value < 0.1.

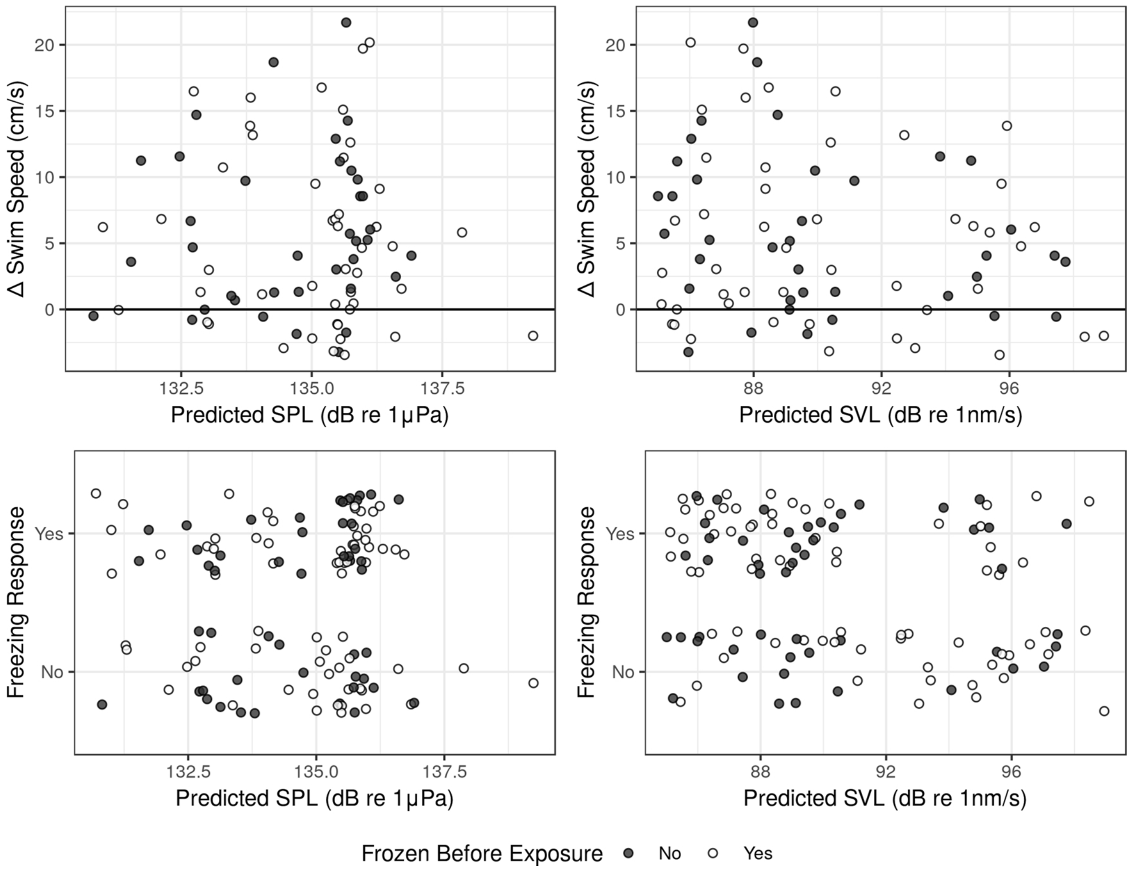

Fig. 5. Interpolated SVL and SPL values at the fast start response locations of all individuals compared to the resulting (top)change in swimming speed averaged over 10 s before and after noise exposure and (bottom) the probability of a freezing response within the 50 s after noise exposure (n = 99). Y-axis variability has been added to the points on the freezing response plots as a visual aid. Mixed effects models revealed that the probability of a freeze response was negatively correlated with SVL. White filled circles indicate instances when the fish was already in a freezing state immediately before the exposure onset.

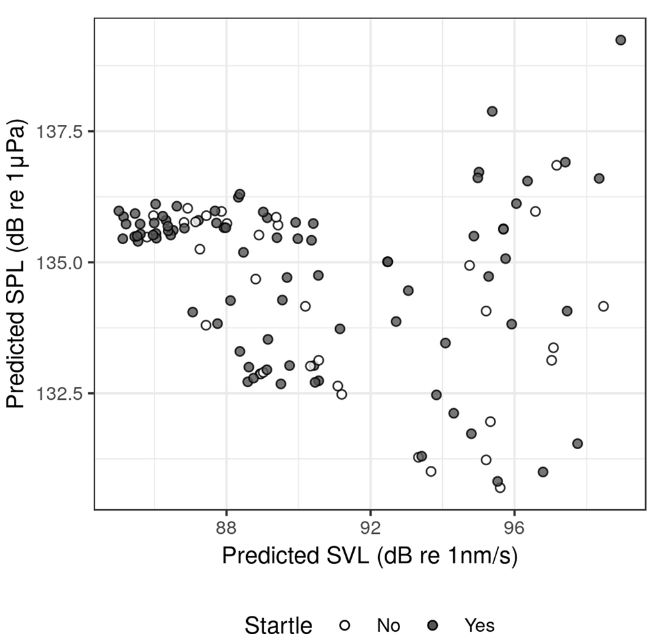

Fig. 6. Occurrence of fast start responses by individuals immediately after sound exposure (n = 128). Grey dots indicate fast start responses to the sound exposure and black dots indicate a lack of response. The interpolated SVL and SPL measurements for the individuals' positions during the onset of sound exposure are indicated on the x-axis and y-axis respectively. No correlation was found between the occurrences of a fast start response and either SVL or SPL estimates.

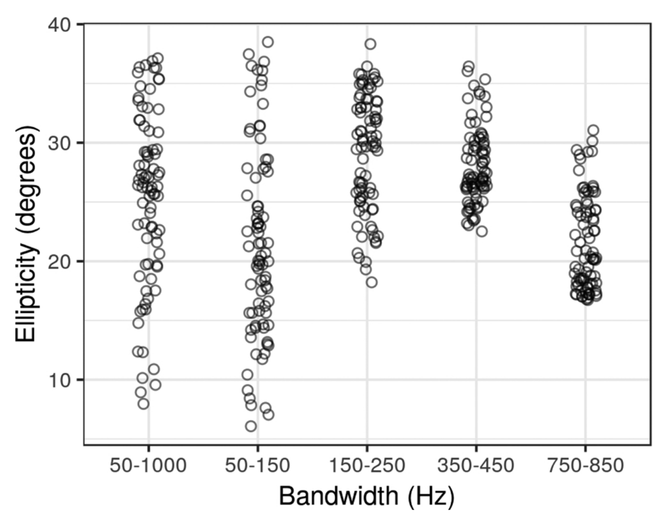

Fig. 7. Particle ellipticity values at the individual's location during the onset of sound exposure (n = 67) predicted by linear interpolation and calculated over different bandwidths. All estimated particle ellipticity values were considerably higher than that which would be expected in ideal far-field conditions from a single sound source (0°). High degrees of particle ellipticity imply a lack of directionality in the underlying particle motion.

4.2. Exploring acoustic sensitivity of fish

The experimental individuals responded to sudden sound bursts of moderate level exposures, similar to previous experiments (Neo et al., 2014; Shafiei Sabet et al., 2015). Behavioural responses were triggered under a wide range in SVL and SPL levels and variable combinations thereof, although no clear correlations between acoustic parameters and the expected behavioural response patterns were observed.

Despite this, one significant correlation between sound and behaviour was observed: the probability of a freezing response was negatively correlated with the SVL at the fish's location during sound exposure. This is in contrast to our expectations as freezing responses, in concert with thrashing and erratic swimming, has been shown to be a reliable indicator of anxiety in the context of light conditions or perceived predation risk (Blaser et al., 2010; Bass and Gerlai, 2008; Cachat et al., 2010) and has also been scored as such in earlier sound impact studies with this species (Shafiei Sabet et al., 2016). Consequently, if SVL was perceptually the most prominent of all sound field features and responsible for a correlation via a causal relationship, one would expect a positive correlation of higher levels with higher probabilities of freezing.

Regardless of the counter-intuitive behavioural response, the experimental set-up employed here yields potential for acoustically induced behavior experiments. Integrating detailed sound field characterization and behavioural assessments of free-swimming fish may yield specific correlations that indicate perceptual prominence for one among multiple audible sound parameters. This will likely remain challenging in small tank environments for a while, as it should be noted that perceptual weighting studies on acoustic parameters of song in birds have only become possible after many years of methodological progress in different laboratories (Dooling and Okanoya, 1995; Beckers et al., 2003; Pohl et al., 2012).

4.3. Methodological potential and problems

As we hope that our study will stimulate follow-up, some methodological potential and problems with the set-up should be addressed. First, it should be noted that swimming restrictions limit natural behavioural response patterns (Calisi and Bentley, 2009; Slabbekoorn 2013; Neo et al., 2016). The analysis of the swimming direction of startle responses presented here yielded no relationship with the direction of the SVL component of the playback sound, except when examining the fish's location at 100 ms after the startle response over a bandwidth of 750–850 Hz. This inconclusive result may be due to the small and rectangular shape of our experimental area where the fish may have preferred to escape in the direction with the largest free area for movement which would cause a bias in escape directions (also see (Shafiei Sabet et al., 2016)).

Secondly, Zebrafish are most sensitive to sound of frequencies around 800 Hz, but are likely to hear up to 3000 Hz (Higgs et al., 2002; Bretschneider et al., 2013). Furthermore, relative sensitivities for particle motion and sound pressure vary spectrally, with fish tending to be relatively more sensitive to particle motion at lower frequencies, as compared to sound pressure (Schulz-Mirbach et al., 2012). Future tests could explore whether sound bursts restricted to relatively low (< 500 Hz) or relatively high (> 1000 Hz) frequencies in the audible range of zebrafish yield differential response patterns with respect to weighting of SVL and SPL. It should be noted that in the current study there were calibration and spatial resolution limitations with regard to the vector sensor, as we were only able to assess particle motion levels within a frequency range of 50–1000 Hz at a relatively low spatial resolution of 9.5 cm (defined by the size of the sensor).

Finally, particle ellipticity may be a relevant feature for acoustic response studies in fish. The predicted levels of ellipticity at the locations of startle responses in this experimental setup were highly variable, dependent on both spatial location and frequency range, and all measured values were considerably higher than what would be expected in far field open water conditions. Although the mechanism for determining directionality is not comprehensively understood in any fish species (Hawkins and Popper, 2018), the capacity for fish to localize a sound source based on the particle motion component of sound fields has been previously shown in the female midshipman (*Porichthys notatus*) (Zeddies et al., 2012). It is expected that higher degrees of particle ellipticity will diminish a fish's ability to localize sound sources, thus reporting measures of particle ellipticity and incorporating them into statistical analysis may be valuable for future studies and provide insight to a lack of observed directional responses.

5. Conclusions

Our findings highlight the importance of reporting particle motion measurements in small tank sound impact studies on fish. This is especially important for small tank studies, as this study has quantitatively shown that particle motion and sound pressure do not share the same relationship in small tanks as they would in open water conditions. Furthermore, we have introduced particle ellipticity as a sound field measurement and possible explanation for a lack of directional response in acoustic response experiments. As this experiment does not provide conclusive results, the relative roles of particle motion, sound pressure, or the ratio between particle velocity and sound pressure (excess SVL) in anxiety-related, sound-induced behaviors requires further study. Despite the unclear results, this study provides an experimental design that leverages the complexity of small tank sound fields to an experimental tool, rather than perceiving it as an obstacle.

The practical challenges for further study are numerous. The lack of standardized methodology, low repeatability, and difficulty in obtaining commercially available geophones and accelerometers still remain obstacles for researchers (Anderson, 2013). Highly complex sound field conditions (Parvulescu, 1964; Akamatsu et al., 2002; Slabbekoorn, 2016; Gray et al., 2016) also remain an issue for indoor studies in fish tanks, as should be clear from this study. Nevertheless, we advocate the exploitation of indoor and outdoor conditions as complementary studies. Furthermore, intensive collaboration among fish biologists, acoustic engineers, and behavioural specialists remains critical for further progress in our fundamental understanding of the acoustic world of both captive and free-ranging fish (Shafiei Sabet et al., 2016; Neo et al., 2016).

Competing interests

The authors declare no competing or financial interests.

Author contributions

J.C. and S.S.S. conducted the experiments. J.C., S.S.S, and H.S. designed the experiments and prepared the manuscript and figures.

Funding

This work was funded by the Iranian Ministry of Science, Research and Technology with the grant number 89100256. S.S.S. was funded by the Iranian Ministry of Science, Research and Technology.

Acknowledgments

We are grateful to Carel ten Cate and the Leiden University Behavioral Biology group members for feedback and invaluable discussions. We would also like to thank Michael Ainslie, Ozkan Sertlek, and Frank Brentschneider for acoustic and analytical advice, and Peter Snelderwaard for advice and assistance with the experimental setup.

References

Ainslie, M.A., 2011. Standard for Measurement and Monitoring of Underwater Noise, Part I: Physical Quantities and their Units. TNO; 2011, September.TNO-DV 2011, The Hague, The Netherlands, pp. C235.

Akamatsu, T., Okumura, T., Novarini, N., Yan, H., 2002. Empirical refinements applicable to the recording of fish sounds in small tanks. J. Acoust. Soc. Am. 112 (6), 3073.

Anderson, P.A., 2013. Acoustic characterization of seahorse tank environments in public aquaria: a citizen science project. Aquac. Eng. 54, 72–77.

Andrew, R.K., Howe, B.M., Mercer, J.A., Dzieciuch, M.A., 2002. Ocean ambient sound: comparing the 1960s with the 1990s for a receiver off the California coast. Acoust. Res. Lett. Online 3, 65–70.

Bass, S.L.S., Gerlai, R., 2008. Zebrafish (Danio rerio) responds differentially to stimulus fish: the effects of sympatric and allopatric predators and harmless fish. Behav. Brain Res. 186 (1), 107–117.

Beckers, G.J.L., Goossens, B.M.A., ten Cate, C., 2003. Perceptual salience of acoustic differences between conspecific and allospecific vocalizations in African collared-doves. Anim. Behav. 65, 605–614.

Blaser, R.E., Chadwick, L., McGinnis, G.C., 2010. Behavioral measures of anxiety in zebrafish (Danio rerio). Behav. Brain Res. 208 (1), 56–62.

Bretschneider, F.A., van den Berg, V., van Veen, H., Teunis, P.F.M., Peters, R.C., 2013. Zebrafish can hear sound pressure and particle motion in a synthesized sound field. Anim. Biol. 63 (2), 199–215.

Cachat, J., Stewart, A., Grossman, L., Gaikwad, S., Kadri, F., Chung, K.M., Wu, M., Wong, K., Roy, S., Suciu, C., Goodspeed, J., Elegante, M., Bartels, B., Elkhayat, S., Tien, D., Tan, J., Denmark, A., Gilder, T., Kyzar, E., DiLeo, J., Frank, K., Chang, K., Utterback, E., Hart, P., Kalueff, A.V., 2010. Measuring behavioral and endocrine responses to novelty stress in adult zebrafish. Nat. Protoc. 5 (11), 1786–1799.

Calisi, R.M., Bentley, G.E., 2009. Lab and field experiments: are they the same animal? Horm. Behav. 56 (1), 1–10.

Craven, A., Carton, A.G., McPherson, C.R., McPherson, G., 2009. Determining and quantifying components of an aquaculture soundscape. J. Aquac. Eng. Fish. Res. 41, 158–165.

Dale, J.J., Gray, M.D., Popper, A.N., Rogers, P.H., Block, B.A., 2015. Hearing thresholds of swimming Pacific bluefin tuna Thunnus orientalis. J. Comp. Physiol. A Neuroethol. Sens. Neural. Behav. Physiol. 201, 441–454.

Dooling, R.J., Okanoya, K., 1995. Psychophysical methods for assessing perceptual categories. In: Klump, G.M., Dooling, R.J., Fay, R.R., Stebbins, W.C. (Eds.), Methods in Comparative Psychoacoustics. Basel: Birkhäuser 307–18.

Fay, R.R., 1984. The goldfish ear codes the axis of acoustic particle motion in three dimensions. Science. 225, 951–954.

Gray, M., Rogers, P.H., Zeddies, D.G., 2016. Acoustic particle motion measurements for bioacousticians: principles and pitfalls. Proc. Meetings Acoust. 27, 010022. https://doi.org/10.1121/2.0000290.

Hawkins, A.D., Popper, A.N., 2018. Directional hearing and sound source localization by fishes. J. Acoust. Soc. Am. 144, 3329.

Higgs, D.M., Souza, M.J., Wilkins, H.R., Presson, J.C., Popper, A.N., 2002. Age- and size-related changes in the inner ear and hearing ability of the adult zebrafish (Danio rerio). J. Assoc. Res. Otolaryngol. 3, 174–184.

Hildebrand, J.A., 2009. Anthropogenic and natural sources of ambient noise in the ocean. Mar. Ecol. Prog. Ser. 395, 5–20.

Horodysky, A.Z., Brill, R.W., 2008. Acoustic pressure and particle motion thresholds in six sciaenid fishes. J. Exp. Biol. 211, 1504–1511.

Kaatz, I.M., Lobel, P.S., 2001. A comparison of sounds recorded from a catfish (Orinocodoras Eigenmanni, Doradidae) in an aquarium and in the field. Biol. Bull. 201, 278–280.

Kunc, H.P., McLaughlin, K.E., Schmidt, R., 2016. Aquatic noise pollution: implications for individuals, populations, and ecosystems. Proceedings of the Royal Society 283. https://doi.org/10.1098/rspb.2016.0839.

Mirjany, M., Preuss, T., Faber, D.S., 2011. Role of the lateral line mechanosensory system in directionality of goldfish auditory evoked escape response. J. Exp. Biol. 214 (20), 3358–3367.

Morris, C.J., Cote, D., Martin, B., Kehler, D., 2018. Effects of 2D seismic on the snow crab fishery. Fish. Res. 197, 67–77.

Nakagawa, S., Schielzeth, H., 2013. A general and simple method for obtaining R2 from generalized linear mixed-effects models. Methods Ecol. Evol. 4 (2), 133–142.

Neo, Y.Y., Seitz, J., Kastelein, R.A., Winter, H.V., ten Cate, C., Slabbekoorn, H., 2014. Temporal structure of sound affects behavioural recovery from noise impact in European seabass. Biol. Conserv. 178, 65–73.

Neo, Y.Y., Hubert, J., Bolle, L., Winter, H.V., ten Cate, C., Slabbekoorn, H., 2016. Sound exposure changes European seabass behaviour in a large outdoor floating pen: effects of temporal structure and a ramp-up procedure. Environ. Pollut. 214, 26–34.

Parvulescu, A., 1964. Problems of propagation and processing. Mar. Bio Acoustics 1, 87–100.

Pohl, N.U., Leadbeater, E., Slabbekoorn, H., Klump, G.M., Langemann, U., 2012. Great tits in urban noise benefit from high frequencies in song detection and discrimination. Anim. Behav. 83 (3), 711–721.

Popper, A.N., Fay, R.R., 1973. Sound detection and processing by teleost fishes: a critical review. J. Acoust. Soc. Am. 53 (6), 1515–1529.

Popper, A., Fay, R., 2011. Rethinking sound detection by fishes. Hear. Res. 273, 25–36.

Popper, A.N., Hastings, M.C., 2009. The effects of anthropogenic sources of sound on fishes. J. Fish Biol. 75, 455–489.

Popper, A.N., Hawkins, A.D., 2018. The importance of particle motion to fishes and invertebrates. J. Acoust. Soc. Am. 143 (1), 470–488.

Radford, A.N., Kerridge, E., Simpson, S.D., 2014. Acoustic communication in a noisy world: can fish compete with anthropogenic noise? Behavioural Ecology. 25, 1022–1030.

Rogers, P.H., Cox, M., 1988. Underwater Sound as a biological stimulus. Sensory Biology of Aquatic Animals. Springer, New York.

Rollo, A.K., Higgs, D., 2008. Differential acoustic response specificity and directionality in the round goby, Neogobius melanostomus. Anim. Behav. 75 (6), 1903–1912.

Schuijf, A., Buwalda, R.J.A., 1975. On the mechanism of directional hearing in cod (Gadus Morhua L.). J. Comp. Physiol. 98 (4), 333–343.

Schulz-Mirbach, T., Metscher, B., Ladich, F., 2012. Relationship between swim bladder morphology and hearing abilities–a case study on Asian and African cichlids. PLoS One 7 (8), e42292.

Shafiei Sabet, S., Neo, Y.Y., Slabbekoorn, H., 2015. The effect of temporal variation in sound exposure on swimming and foraging behaviour of captive zebrafish. Anim. Behav. 107, 49–60.

Shafiei Sabet, S., Wesdorp, K., van Dooren, D., Slabbekoorn, H., 2016. Sound affects behavior of captive zebrafish: always consider the potential for acoustic effects on your laboratory tests. Proceedings of Meetings on Acoustics 27, 010010.

Simpson, S.D., Purser, J., Radford, A.N., 2015. Anthropogenic noise compromises anti-predator behaviour in European eels. Glob. Change Biol. 21, 586–593.

Simpson, S.D., Radford, A.N., Nedelec, S.L., Ferrari, M.C.O., Chivers, D.P., McCormick, M.I., Meekan, M.G., 2016. Anthropogenic noise increases fish mortality by predation. Nat. Commun. 7, 10544.

Slabbekoorn, H., 2016. Aiming for Progress in Understanding Underwater Noise Impact on Fish: Complementary Need for Indoor and Outdoor Studies. The Effects of Noise on Aquatic Life. pp. 1–10.

Slabbekoorn, H., Bouton, N., van Opzeeland, I., Coers, A., ten Cate, C., Popper, A.N., 2010. A noisy spring: the impact of globally rising underwater sound levels on fish. Trends Ecol. Evol. 25, 419–427.

Williams, R., Wright, A.J., Ashe, E., Blight, L.K., Bruintjes, R., Canessa, R., Clark, C.W., Cullis-Suzuki, S., Dakin, D.T., Erbe, C., Hammond, P.S., Merchant, N.D., O'Hara, P.D., Purser, J., Radford, A.N., Simpson, S.D., Thomas, L., Wale, M.A., 2015. Impacts of anthropogenic noise on marine life: publication patterns, new discoveries, and future directions in research and management. Ocean Coast. Manag. 115, 17–24.

Wysocki, L.E., Codarin, A., Ladich, F., Picciulin, M., 2009. Sound pressure and particle acceleration audiograms in three marine fish species from the Adriatic Sea. J. Acoust. Soc. Am. 126 (4), 2100–2107.

Zeddies, D.G., Fay, R.R., Gray, M.D., Alderks, P.W., Acob, A., Sisneros, J.A., 2012. Local acoustic particle motion guides sound-source localization behavior in the plainfin midshipman fish, Porichthys notatus. J. Exp. Biol. 215 (1), 152–160.